FusB Energizes Import across the Outer Membrane through Direct Interaction with Its Ferredoxin Substrate

Marta Wojnowska,[a] Daniel Walker[a]

[a]Institute of Infection, Immunity and Inflammation, College of Medical, Veterinary and Life Sciences, University of Glasgow, Glasgow, United Kingdom

ABSTRACT Phytopathogenic *Pectobacterium* spp. import ferredoxin into the periplasm for proteolytic processing and iron release via the ferredoxin uptake system. Although the ferredoxin receptor FusA and the processing protease FusC have been identified, the mechanistic basis of ferredoxin import is poorly understood. In this work, we demonstrate that protein translocation across the outer membrane is dependent on the TonB-like protein FusB. In contrast to the loss of FusC, loss of FusB or FusA abolishes ferredoxin transport to the periplasm, demonstrating that FusA and FusB work in concert to transport ferredoxin across the outer membrane. In addition to an interaction with the "TonB box" region of FusA, FusB also forms a complex with the ferredoxin substrate, with complex formation required for substrate transport. These data suggest that ferredoxin transport requires energy transduction from the cytoplasmic membrane via FusB both for removal of the FusA plug domain and for substrate translocation through the FusA barrel.

IMPORTANCE The ability to acquire iron is key to the ability of bacteria to cause infection. Plant-pathogenic *Pectobacterium* spp. are able to acquire iron from plants by transporting the iron-containing protein ferredoxin into the cell from proteolytic processing. In this work, we show that the TonB-like protein FusB plays a key role in transporting ferredoxin across the bacterial outer membrane by directly energizing its transport into the cell. The direct interaction of the TonB-like protein with substrate is unprecedented and explains the requirement for the system-specific TonB homologue in the ferredoxin uptake system. Since multiple genes encoding TonB-like proteins are commonly found in the genomes of Gram-negative bacteria, this may be a common mechanism for the uptake of atypical substrates via TonB-dependent receptors.

KEYWORDS *Pectobacterium*, TonB, ferredoxin, outer membrane, plant pathogens, plant-microbe interactions, protein transport

Gram-negative bacteria have evolved a number of strategies for the acquisition of iron and other nutrients in which "TonB-dependent" transporters (TBDTs) play a central role (1). In the case of siderophore-mediated iron acquisition, the iron-siderophore complex is imported into the cell, captured by a siderophore-specific periplasmic binding protein, and delivered to an ABC transporter for importation into the cytoplasm (2). For iron acquisition from large host proteins such as transferrin, the iron-containing protein is captured at the cell surface through TBDT binding and the iron stripped and subsequently transported through the lumen of the TBDT (3). In addition to the outer membrane (OM) receptor, whose lumen constitutes the translocation route, TBDT-mediated transport requires a complex of three proteins anchored in the inner membrane: TonB, ExbB, and ExbD (4, 5). The ExbBD-TonB complex enables the entry of the nutrient by removal of a force-labile portion of the plug domain, which obstructs the receptor lumen (6). ExbB and ExbD are related to the flagellar motor proteins and harness proton motive force (PMF) to energize the transport process.

In addition to the uptake of iron siderophores and other metal chelating com-

pounds such as vitamin B12, TBDTs also transport complex carbohydrates and simple sugars (7). A recent study also described the role of a TonB-dependent receptor in protein export, suggesting that TonB-dependent receptors are highly adaptable to the transport of diverse substrates across the OM (8). The flexibility in the range of substrates that are amenable to transport by TBDTs is exploited by protein antibiotics such as colicins and pyocins that use TBDTs as their primary cell surface receptor and translocator (9). As with the uptake of nutrients, translocation of colicins and pyocins via TBDTs is PMF dependent, although the periplasm-spanning protein TonB is required in such cases both to remove the force-labile region of the TBDT-plug domain and subsequently to energize protein translocation across the OM (10). Protein translocation occurs by direct interaction with an N-terminal intrinsically unstructured region of the toxin that, similarly to the TBDTs, carries a TonB-binding motif (10).

We recently demonstrated that TBDT-mediated iron acquisition from the iron-sulfur cluster containing protein ferredoxin represents an unprecedented example of protein translocation into the bacterial cell for nutrient acquisition (11). Ferredoxin binding at the cell surface is mediated by the TBDT FusA protein, and, following transport of intact ferredoxin into the periplasm, the substrate is subjected to proteolytic processing by the M16 protease FusC (11, 12). Cleavage by FusC results in release of the iron-sulfur cluster and is required for effective iron acquisition from ferredoxin by *Pectobacterium*. Together with the genes encoding FusA and FusC, the Fus operon contains two additional genes, with *fusB* encoding a TonB homologue and *fusD* a putative ABC transporter (12). Interestingly, the M-type pectocins M1 and M2, which we have previously described, parasitize the ferredoxin uptake system through an N-terminal ferredoxin domain that is highly homologous to plant ferredoxin domains (13, 14).

More recently, the X-ray structure of FusC bound to ferredoxin has been reported, showing that substrate recognition occurs at a site distant from the active site (15). Furthermore, only parts of the ferredoxin molecule are visible in the structure, implying that the bound substrate is largely present in an unstructured form. On the basis of these data, it was suggested that ferredoxin transport occurs by means of a Brownian ratchet mechanism in which FusC acts as a periplasmic anchor to facilitate translocation of ferredoxin across the OM via the lumen of FusA (12, 15). Similar mechanisms have been postulated to account for mitochondrial protein uptake, whereby cytoplasmically synthesized proteins are translocated via the TOM and TIM23 complexes (16, 17). As such, this would represent a hitherto-unexpected evolutionary link between mitochondrial and plastid protein import and bacterial protein import via the Fus uptake system (FUS) and other postulated protein uptake systems.

In this work, we show that FusC does not facilitate ferredoxin import and that, like the import of other TBDT substrates, ferredoxin uptake is PMF dependent. Instead, we show that the TonB homologue encoded within the *fus* operon, FusB, is required for ferredoxin import and that the mechanism of ferredoxin import involves a direct interaction between FusB and the ferredoxin substrate. The evidence pointing to a direct interaction of the TonB-like protein with the substrate is unprecedented and explains the requirement for the system-specific TonB homologue in the Fus system. Our data also show that, in addition to the direct interaction with the substrate, FusB fulfils another role—similarly to other TonB proteins—in interacting with the "TonB box" of FusA for plug displacement. Since multiple genes encoding TonB-like proteins are commonly found in the genomes of Gram-negative bacteria, this may be a common mechanism for the uptake of atypical substrates via TonB-dependent receptors.

RESULTS

Ferredoxin import is independent of FusC but requires proton motive force.
We previously showed that FusC is a highly specific protease that targets plant ferredoxin to release iron from this host protein in the periplasm of *Pectobacterium* spp. (11). However, it has also been suggested that FusC plays an additional role in iron acquisition through a direct involvement in ferredoxin transport across the outer membrane by means of a Brownian ratchet mechanism, specifically acting as a periplas-
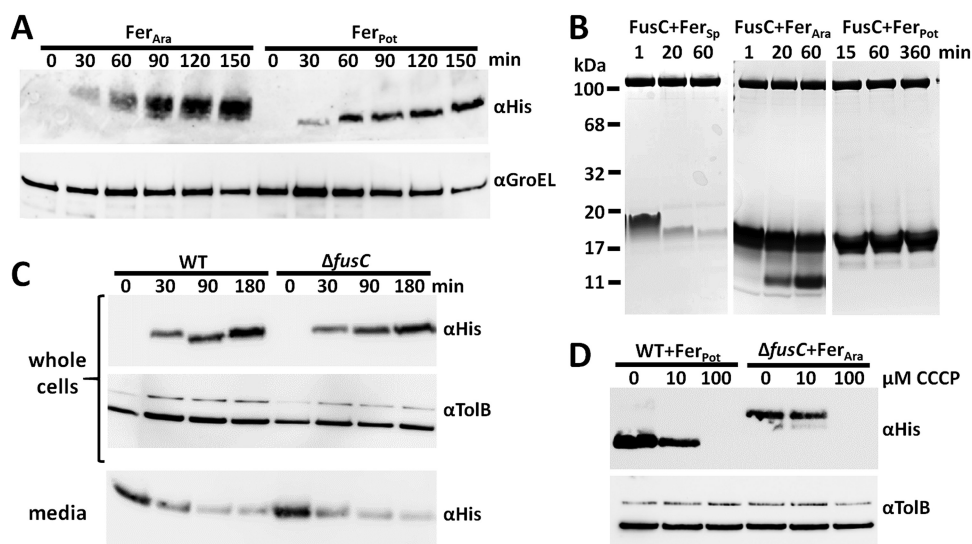
FIG 1 Import of ferredoxin is FusC independent and requires proton motive force. (A) Uptake of His-tagged Fer_{Ara} and Fer_{Pot} by $\Delta fusC$ cells over time determined by immunoblotting of whole-cell extracts. GroEL served as the loading control. (B) FusC-mediated cleavage assays of plant ferredoxins. Comparable cleavage rates were observed in >5 independent experiments. (C) Comparison of levels of Fer_{Pot} uptake by wild-type (WT) and $\Delta fusC$ cells, with TolB as the loading control. The bottom panel shows the concomitant depletion of ferredoxin from the media. (D) Ferredoxin import assays in the presence of protonophore CCCP. Fer_{Pot} was used as a reporter in wild-type cells, while Fer_{Ara} was used in $\Delta fusC$ cells. TolB served as the loading control.

mic anchor (15). Our own previous work suggests that if FusC does play a role in ferredoxin import, this role is not essential since the accumulation of *Arabidopsis* ferredoxin can still be observed in a *Pectobacterium carotovorum* LMG2410 (*Pc*LMG2410) strain lacking FusC (11). However, using *Arabidopsis* ferredoxin (Fer_{Ara}), it is not possible to directly compare the rates and extents of ferredoxin uptake between wild-type (WT) and $\Delta fusC$ *P. carotovorum* since Fer_{Ara} is cleaved by FusC upon importation into the periplasm in the WT strain; hence, on the basis of these data, we could not rule out a possible role for FusC in ferredoxin import.

To test the hypothesis that FusC facilitates translocation of ferredoxin to the periplasm, we compared the levels of uptake of potato ferredoxin (Fer_{Pot}) in wild-type and $\Delta fusC$ *Pc*LMG2410. Fer_{Pot} was used as we had observed that although, similarly to Fer_{Ara}, it can be transported into cells (Fig. 1a), unlike Fer_{Ara} and spinach ferredoxin (Fer_{Sp}), both of which support robust growth of *Pc*LMG2410 under iron-limiting conditions (12, 13), it is not cleaved at an appreciable rate by FusC and so accumulates intracellularly in wild-type *Pc*LMG2410 (Fig. 1b). To compare the levels of uptake of Fer_{Pot} in wild-type and $\Delta fusC$ *Pc*LMG2410, cells were grown under iron-limiting conditions through the addition of the iron chelator 2,2'-bipyridine and were supplemented with Fer_{Pot}. The amount of Fer_{Pot} in whole-cell extracts and in the media was determined by immunoblotting. Levels of Fer_{Pot} obtained from cell extracts increased at the same rate in whole-cell extracts, and rates of removal of ferredoxin from the media were similar (Fig. 1c). These data show that FusC does not play a role in protein import and that the role of FusC in iron acquisition is likely restricted to proteolytic processing of ferredoxin as we previously reported (11).

To further probe the mechanism of ferredoxin uptake, we tested the ability of *Pc*LMG2410 cells to accumulate Fer_{Pot} under iron-limiting conditions and in the presence of the uncoupling agent carbonyl cyanide m-chlorophenylhydrazone (CCCP), which dissipates the PMF through transport of protons across the cytoplasmic membrane (18). The intracellular accumulation of Fer_{Pot} by *Pc*LMG2410 was markedly reduced in the presence of 10 μM CCCP, relative to cells grown in the absence of the uncoupling agent, and was abolished in the presence of 100 μM CCCP (Fig. 1d). Similar effects resulting from the action of CCCP were observed on the intracellular accumulation of *Arabidopsis* ferredoxin by $\Delta fusC$ LMG2410 (Fig. 1d). These data show that,
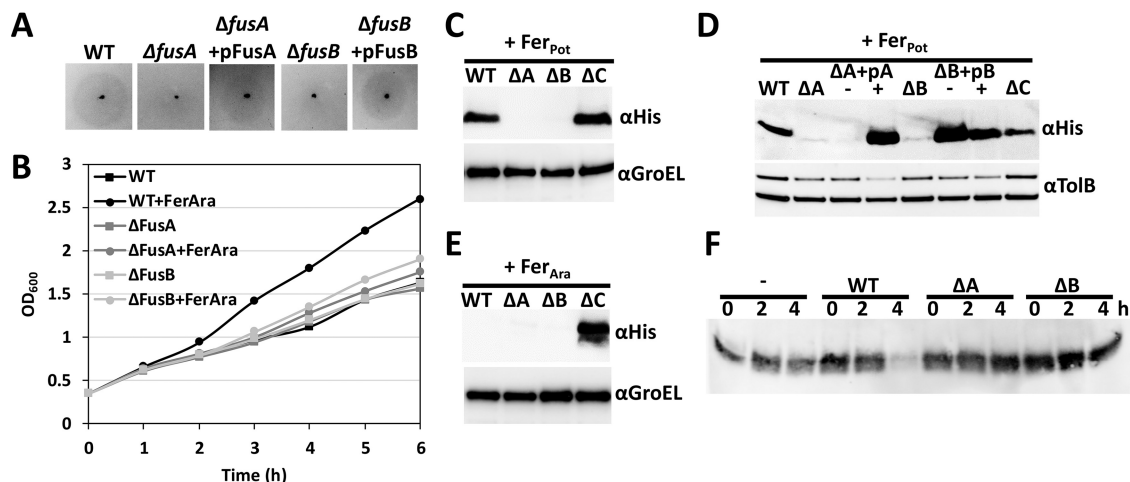
FIG 2 FusA and FusB are required for ferredoxin uptake. (A) Growth enhancement assay using spinach ferredoxin spotted onto a soft-agar overlay containing the wild-type (WT) strain, deletion strains, and deletion strains recomplemented in *trans* with the respective plasmids. Similar phenotypes were observed in 5 independent assays. (B) Growth curve comparing the rates of growth of the wild-type strain and each deletion strain in the absence and presence of *Arabidopsis* ferredoxin. Comparable rates were observed in 3 independent experiments. (C) Internalization assay of Fer_{Pot}. Mid-log-phase cells of each strain were supplemented with 2,2′-bipyridine and 1 μM ferredoxin and grown for 1 h, and whole-cell extracts were probed with anti-His antiserum for His-tagged Fer_{Pot}. GroEL served as the loading control. (D) Internalization assay of His-tagged Fer_{Pot}, including deletion strains recomplemented in *trans* using plasmids harboring the corresponding genes. ΔA+pA, Δ*fusA* plus pFusA; ΔB+pB, Δ*fusB* plus pFusB. Prior to the addition of 2,2′-bipyridine and ferredoxin, the cultures of recomplemented strains were split in two and either supplemented with 0.5 mM IPTG ("+") or grown in the absence of inducer ("-"). TolB served as the loading control. (E) Internalization assay using His-tagged Fer_{Ara} (see panel C). (F) Depletion assay showing the gradual reduction in the level of *Arabidopsis* ferredoxin in the media derived from uninoculated (-), wild-type, Δ*fusA* (ΔA), and Δ*fusB* (ΔB) cell cultures.

analogously to other TBDT-mediated transport processes (10, 19), the import of ferredoxin is PMF dependent and a Brownian ratchet mechanism is unlikely to play a key role in ferredoxin import in *Pectobacterium* spp.

FusB mediates ferredoxin import into the periplasm. As we previously reported, in addition to *fusA* and *fusC*, the Fus operon carries genes that encode a TonB homologue, FusB, and an ABC transporter, FusD (12). Given the documented role of TonB in siderophore import in many bacterial species, we supposed that FusB might play a similar role in protein import, having perhaps evolved additional functionality required to mediate the passage of a large substrate through the lumen of the TBDT FusA. To test this hypothesis, we created Δ*fusA* and Δ*fusB* strains in *Pc*LMG2410 and initially probed them using growth enhancement assays under iron-limiting conditions. As indicated by the loss of growth enhancement both on solid media (Fig. 2a) and in liquid culture (Fig. 2b), these two genes encode proteins which are essential for Fus-mediated iron acquisition. The possibility that deletion of either gene affected the expression or level of FusC and thus indirectly affected the growth enhancement phenotype was ruled out by immunoblotting whole-cell extracts with anti-FusC antiserum (see Fig. S1 in the supplemental material). We further investigated the ability of the Δ*fusA* and Δ*fusB* *Pc*LMG2410 mutant strains to import ferredoxin relative to wild-type and Δ*fusC* strains using Fer_{Pot}, which cannot be cleaved by FusC. Consistent with the hypothesized role of FusB in protein import, and in contrast to the wild-type and Δ*fusC* strains, we did not observe intracellular accumulation of Fer_{Pot} in Δ*fusA* and Δ*fusB* *Pc*LMG2410 (Fig. 2c). The ferredoxin import phenotype lost in the Δ*fusA* and Δ*fusB* strains was restored by plasmid-based complementation of *fusA* and *fusB*, respectively (Fig. 2d). In these experiments, the production of FusA and FusB was inducible by the use of IPTG (isopropyl-β-D-thiogalactopyranoside) under the control of the T5 promoter, although in the case of FusB complementation, leaky expression in the absence of IPTG is sufficient to restore protein import.

To ensure that the abrogation of substrate import is not specific to Fer_{Pot}, we also monitored the ability of the Δ*fusA* and Δ*fusB* strains to utilize Fer_{Ara}. However, for this

substrate, instead of measuring intracellular ferredoxin accumulation, we determined loss of ferredoxin from the growth media, since accumulation of Fer_{Ara} was observed only in the LMG2410 $\Delta fusC$ strain (Fig. 2e). Consistent with the internalization assay and growth enhancement assays, the ferredoxin content of the media decreased over time in the presence of wild-type cells but not in the presence of the $\Delta fusA$ and $\Delta fusB$ strains, indicating that both FusA and FusB are required for Fer_{Ara} uptake (Fig. 2f). To exclude the possibility that the increased depletion of ferredoxin from the media in the wild-type cultures was due to the higher growth rate of this strain than of the $\Delta fusA$ and $\Delta fusB$ strains in the presence of Fer_{Ara}, we directly compared levels of Fer_{Ara} depletion from the media using the $\Delta fusA$ and $\Delta fusC$ strains (Fig. S2), as neither of these strains shows a ferredoxin-dependent growth enhancement. Over 7 h, Fer_{Ara} was gradually depleted from the media by the $\Delta fusC$ strain and accumulated in the cells, as indicated by immunoblots of whole-cell extracts obtained at the end of the assay. In contrast, the level of Fer_{Ara} in the media of the $\Delta fusA$ strain remained unchanged and no ferredoxin was detected in whole-cell extracts, providing further evidence that deletion of $fusA$ (and $fusB$) abrogates the import of Fer_{Ara}.

FusB directly interacts with the TonB box of FusA. Having determined that the TonB-like protein FusB is required for ferredoxin import, we aimed to elucidate the mechanism of ferredoxin uptake. Analysis of the FusA sequence showed the presence of a putative TonB box, DTILVRST, with a sequence similar to that of TonB boxes from well-characterized *Escherichia coli* TBDTs and other *Pc*LMG2410 TBDTs (Fig. S3). The functional importance of this putative TonB box region was demonstrated using ferredoxin import assay and plasmid-based complementation of the $\Delta fusA$ strain, which showed that proline substitutions within the putative TonB box abolished internalization of the FusA substrate ferredoxin (Fig. S4). The similarity of the TonB box of FusA to the TonB boxes of other *Pc*LMG2410 and *E. coli* TBDTs suggests that FusA may interact with *Pc*LMG2410 TonB and not with FusB. Although *Pc*LMG2410 has 6 genes that encode TonB-like proteins, we hypothesized that the protein that was most similar to *E. coli* TonB, and that we refer to here as *Pc*TonB, would fulfil the same function as this protein in servicing multiple TBDTs, with the primary function of dislocating the plug domain to enable substrate transport.

To determine if TonB or FusB or both TonB and FusB interact directly with FusA, we produced a construct consisting of the N-terminal region of FusA (residues 21 to 66), excluding the signal peptide region, fused to green fluorescent protein (GFP) ($FusA_{NTR}$-GFP) and determined if this interacts with the isolated C-terminal domains of *Pc*TonB ($TonB_{CTD}$) and FusB ($FusB_{CTD}$) by isothermal titration calorimetry (ITC). Clearly identifiable heat data representing binding were observed on titration of $FusA_{NTR}$-GFP into $FusB_{CTD}$, although the affinity of $FusB_{CTD}$ for $FusA_{NTR}$-GFP is weak (57 μM) (Fig. 3a). No heat data representing binding were observed on titration of isolated GFP into $FusB_{CTD}$ (Fig. S5), showing that the C-terminal domain of FusB specifically interacts with the N-terminal region of FusA. Interestingly, similar heat data representing binding were observed on titration of $FusA_{NTR}$-GFP into $TonB_{CTD}$ (Fig. S6), demonstrating that the N-terminal region of FusA can also interact with *Pc*TonB.

To determine if the *Pc*TonB plays a role in ferredoxin uptake, we deleted the corresponding gene in *Pc*LMG2410 and tested the growth enhancement phenotype of this strain in the presence of Fer_{Sp}. In contrast to deletion of $fusB$, the loss of $tonB$ did not reduce the growth enhancement phenotype (Fig. 3b); in fact, the $\Delta tonB$ strain showed zones of growth enhancement in the presence of Fer_{Sp} that were more prominent than those seen with the wild-type strain and showed increased intracellular accumulation of Fer_{Pot} relative to wild-type *Pc*LMG2410 (Fig. 3c). However, *Pc*LMG2410 $\Delta tonB$ exhibited poor growth in the presence of 2,2′-bipyridine relative to the wild-type strain (Fig. 3d), with very faint growth observable after 24 h. These data indicate that, although *Pc*TonB does play the expected generic role in iron uptake, this does not include iron acquisition from ferredoxin. Furthermore, despite the aforementioned observation that TonB interacts with FusA *in vitro* (and possibly *in vivo*), this interaction
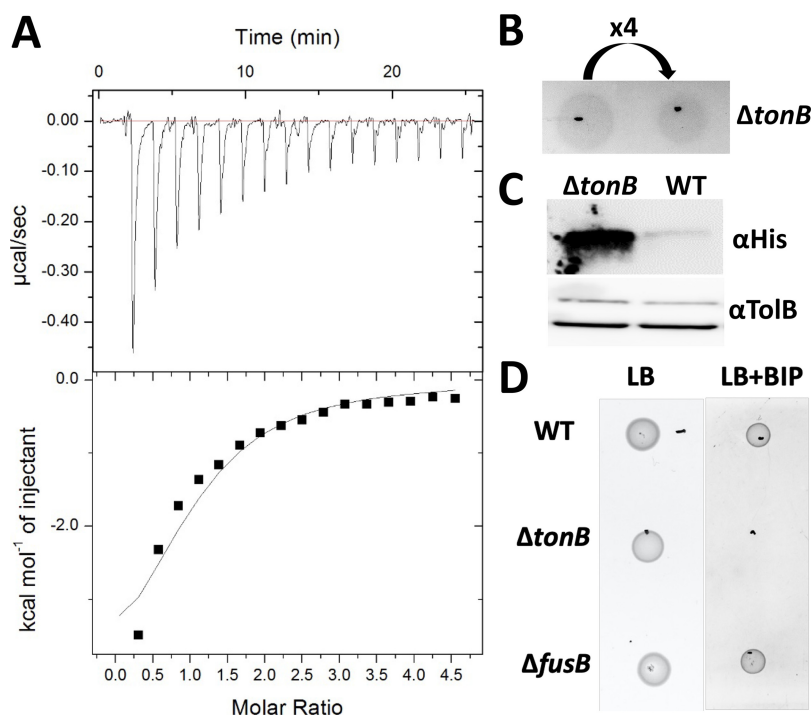
FIG 3 FusB interacts with the FusA "TonB box" and, unlike *Pc*TonB, is required for ferredoxin uptake. (A) ITC binding isotherm of 1 mM $FusA_{NTR}$-GFP titrated into 90 μM $FusB_{CTD}$. The calculated K_d for the $FusA_{NTR}$-GFP-$FusB_{CTD}$ complex is 57 ($\pm$12) μM ($n = 3$). (B) Growth enhancement assay using spinach ferredoxin on soft-agar overlay containing $\Delta tonB$ cells. "x4" refers to the dilution factor. The experiment was repeated 5 times with comparable outcomes. (C) Uptake of His-tagged potato ferredoxin by $\Delta tonB$ and wild-type cells. Whole-cell extracts obtained after 1 h by incubation of each cell type with ferredoxin were probed with anti-His antiserum. TolB served as the loading control. The experiment was performed 4 times with comparable results. (D) Growth assay of wild-type (WT), $\Delta tonB$, and $\Delta fusB$ cells spotted onto LB agar (LB) or LB agar supplemented with 400 μM 2,2'-bipyridine (LB+BIP). Comparable phenotypes were observed in two independent experiments.

is not sufficient for ferredoxin uptake. Indeed, there may be competition between FusB and TonB for complex formation with FusA, with only the FusB-FusA complex being productive with respect to ferredoxin uptake.

FusB interacts directly with the ferredoxin substrate. The ability of FusB and *Pc*TonB to interact with FusA, but with only the former able to mediate ferredoxin uptake, suggests that FusB plays an additional role essential for ferredoxin import. One possibility is that FusB directly interacts with the protein substrate after the initial binding of ferredoxin to FusA at the cell surface. To test this, we sought to determine if ferredoxin forms a complex with the isolated C-terminal domain of FusB by size exclusion chromatography (SEC). SEC of ferredoxin mixed with $FusB_{CTD}$ monitored at 280 nm and 330 nm gave a peak that indicated the presence of a species of higher molecular weight than $FusB_{CTD}$ or Fer_{Sp} alone, providing evidence of complex formation (Fig. 4a). We further investigated the formation of the $FusB_{CTD}$-Fer_{Sp} complex by isothermal titration calorimetry, titrating Fer_{SP} into $FusB_{CTD}$ (Fig. 4b). These data show that FusB interacts directly with the ferredoxin substrate. In contrast, no complex formation was observed between ferredoxin and the purified C-terminal domain of TonB ($TonB_{CTD}$) using SEC (Fig. 4c).

Inspection of the amino acid sequence of FusB shows that the N-terminal portion of the predicted globular domain and the preceding linker contained a significant number of positively charged amino acids; such amino acids were absent from *Pc*LMG2410 and *E. coli* proteins (Fig. S7). Two such residues (Arg176 and Arg177) were found in place of the highly conserved Gln-Pro-Gln residues, which form a part of the BtuB TonB box binding motif (QPQYP) in *E. coli* TonB [20]. This arginine motif is located within a loop/linker region of TonB proteins, connecting the periplasm-spanning and globular
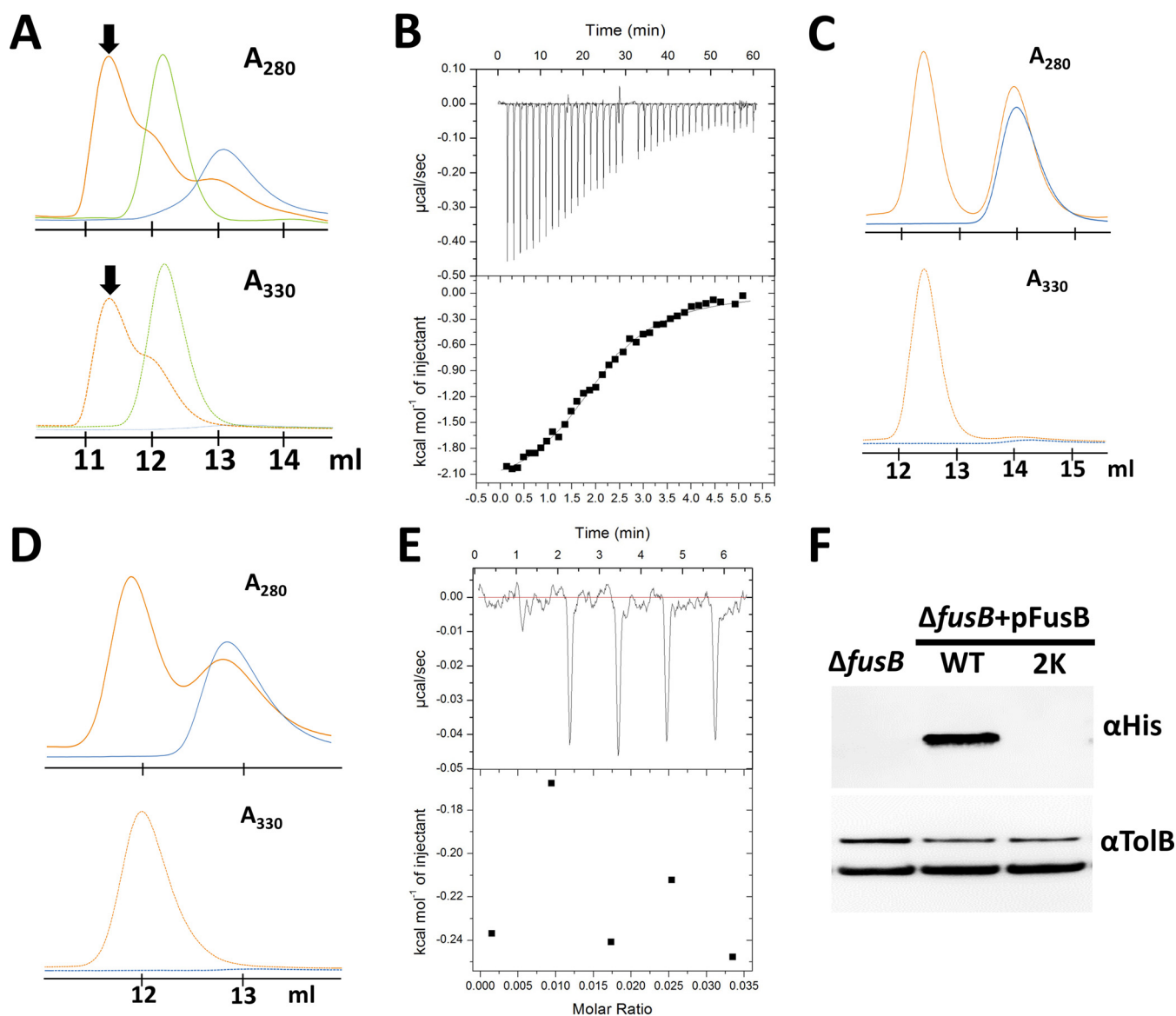
FIG 4 FusB interacts with ferredoxin substrate. (A) Overlaid size exclusion chromatograms of FusB$_{CTD}$ (blue) and spinach ferredoxin (green) and a mixture of the two proteins (orange), with the arrows pointing at the ferredoxin-FusB$_{CTD}$ complex. Similar results were obtained from 5 independent runs. (B) ITC binding isotherm of 600 μM Fer$_{Sp}$ titrated into 70 μM FusB$_{CTD}$. The calculated K_d value for the Fer$_{Sp}$-FusB$_{CTD}$ complex is 8.7 ($\pm$3.5) μM (n = 3). (C) TonB$_{CTD}$ does not form a complex with ferredoxin. Overlay of size exclusion chromatograms shows TonB$_{CTD}$ in the absence (blue trace) and in the presence (orange trace) of Fer$_{Sp}$. (D) Size exclusion chromatograms (280 and 330 nm) of FusB$_{CTD}$ R176K/R177K alone (blue) or in the presence of spinach ferredoxin (orange) showing no complex formation. (E) ITC titration of Fer$_{Sp}$ into FusB$_{CTD}$ R176K/R177K showing only heat data correlating to dilution. (F) Ferredoxin import assay showing the level of uptake of His-tagged potato ferredoxin by $\Delta fusB$ cells complemented with plasmids encoding either wild-type (WT) or FusB$_{CTD}$ R176K/R177K (2K). The experiment was performed 2 times.

domains. Substitution of the two FusB$_{CTD}$ arginine residues with lysines rendered a folded protein that did not comigrate with ferredoxin in SEC (Fig. 4d), and no heat data representing binding were detected by ITC on titration of Fer$_{Sp}$ into FusB$_{CTD}$ R176K/R177K (Fig. 4e). Similarly, *Pc*LMG2410 $\Delta fusB$ could not be complemented with a pFusB plasmid encoding the FusB R176K/R177K variant (Fig. 4f). Therefore, at least one of these two arginine residues appears to be critical for FusB-substrate interaction.

DISCUSSION

Our recent discovery that ferredoxin is imported into the periplasm of *P. carotovo-rum* revealed an unprecedented example of protein uptake for nutrient acquisition in Gram-negative bacteria (11). In this work, we define key aspects of the mechanism of

ferredoxin transport across the outer membrane. In a recent report, it was hypothesized that the M16 protease FusC acts as a periplasmic anchor that facilitates ferredoxin uptake by means of Brownian-ratchet mechanism (15). However, the data presented here are inconsistent with this model, showing that ferredoxin import is independent of FusC. Instead, ferredoxin uptake requires energy transduction from the PMF and the TonB-like protein FusB. Therefore, the mechanism of ferredoxin import shares some similarity with the mechanism of import of widely studied substrates of TBDTs, such iron siderophores and vitamin B12 (4, 21). For these substrates, according to the currently accepted models of TonB-dependent transport, the major role of TonB is in the displacement or partial displacement of the plug domain from their specific TBDTs (6, 10).

Interestingly, in the case of FusA, both FusB and PcTonB are able to interact with its N-terminal region and so both these proteins may be able to facilitate displacement of the FusA plug domain. However, deletion of the genes encoding the two TonB proteins showed that only FusB is essential for ferredoxin transport, demonstrating an additional role for FusB in this process that cannot be fulfilled by PcTonB. Although the affinity of $FusB_{CTD}$ for $FusA_{NTR}$ is low (57 μM), comparable complexes showing low affinity between TBDT TonB-binding peptides and TonB proteins have been previously described. For example, the affinity reported for the TonB-like protein HasB interaction with a 21-mer HasR N-terminal peptide was 25 μM (22). Similarly weak interactions between TonB and TBDT TonB box peptides have been reported for FhuA (36 μM) (23) and BtuB (9.4 μM) (6). However, complex formation between TonB and TonB-binding peptides is characterized by β-strand augmentation, which is known to result in the formation of mechanically strong complexes (6). Indeed, it has been demonstrated in vitro using atomic force microscopy that the TonB-BtuB Ton box complex is sufficiently mechanically robust to induce partial unfolding of the BtuB plug domain, forming a channel through which the vitamin B12 substrate can translocate (6).

The ability of FusB to form a complex with ferredoxin, which PcTonB lacks, indicates that this additional role involves the direct interaction of FusB with the ferredoxin substrate and that this complex formation is essential for ferredoxin transport through the lumen of FusA. Consistent with this, we identified an arginine motif that is required for FusB-mediated ferredoxin uptake by $P.$ $carotovorum$ and formation of the FusB-ferredoxin complex. Our current model of Fus-mediated iron acquisition, whereby FusB fulfils two distinct roles, is schematically shown in Fig. 5. In this model, binding of the substrate on the extracellular side of FusA releases the TonB box into the periplasmic space, where it is captured by FusB. Due to the dimensions of the globular ferredoxin, which are similar to those of the lumen of its FusA TBDT (11), ferredoxin is unlikely to be able to readily diffuse into the periplasm after removal of the FusA plug domain. We therefore hypothesize that the interaction of FusB with the substrate involves a further PMF-dependent step required to pull the ferredoxin substrate through the lumen of FusA. This would involve the C-terminal domain of FusB, which is of a size comparable to those of plant ferredoxins, entering the lumen of FusA to contact ferredoxin on the cell surface. The FusB-ferredoxin complex would then be able to be pulled into the periplasm, using the ExbBD complex and PMF, after which the substrate would be processed by FusC. Although we present a model relying on a single FusB protein per import cycle, we cannot exclude the possibility that the removal of the FusA plug and ferredoxin import would involve two separate FusB molecules.

The occurrence of genes encoding multiple TonB-like proteins is a common feature of many Gram-negative bacteria (24), and specific TonB proteins are required in some cases for the uptake of specific substrates, as in the case of TonB2 of $Vibrio$ $anguillarum$ for anguibactin uptake (25), while other cases exhibit some level of functional redundancy (26). However, to our knowledge the Fus system represents the only substrate import system in which a TonB protein has been shown to directly interact with the substrate. This additional functionality displayed by FusB may reflect the nature of the ferredoxin substrate, which is atypically large in comparison to the well-studied TBDT siderophore substrates. In this respect, the uptake of ferredoxin is similar to the
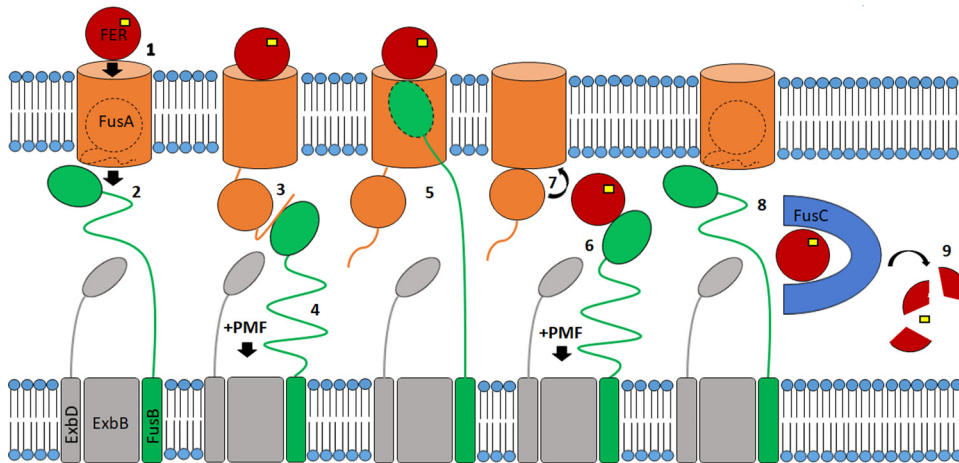
FIG 5 Proposed mechanism of FUS-mediated ferredoxin import mechanism. In the proposed mechanism, FusB (green) fulfils two roles, first, in displacement of the FusA plug domain, and, second, in directly mediating ferredoxin translocation via the FusA lumen. Binding of ferredoxin (red) to FusA at the cell surface (step 1) causes release of the FusA TonB box into the periplasm (step 2), where it is bound by FusB, which dislocates the plug domain (step 3) through energy transduced from the PMF via the ExbBD complex (step 4). FusB is then able to enter the lumen of FusA and bind ferredoxin (step 5) and, through transduction of the PMF, translocate ferredoxin into the periplasm (step 6). The plug domain is then able to reenter the FusA barrel (step 7) and return the FusA and FusB proteins to their resting states. Ferredoxin is then bound by FusC in the periplasm (step 8), which proteolytically cleaves the substrate, releasing the iron-sulfur cluster (yellow) (step 9).

TonB-dependent uptake of the colicins and pyocins, which directly interact with TonB after threading their TonB box-containing intrinsically unstructured translocation domain (IUTD) though the lumen of the corresponding TBDT (10, 27). However, since plant ferredoxins are highly stable proteins that lack any kind of similar unstructured regions, our hypothesis is that in order to contact ferredoxin, FusB must enter the FusA lumen and contact FusA-bound substrate at the cell surface. This proposed mechanism also explains why the ferredoxin-containing bacteriocins do not require an IUTD that contains a TonB box to cross the *P. carotovorum* outer membrane, with FusB proteins able to directly contact their ferredoxin receptor-binding domains at the cell surface, thus enabling parasitization of the Fus system (12, 14).

In summary, we describe a novel mechanism of TonB-dependent nutrient uptake that requires a direct interaction between the substrate and the cognate TonB protein. The occurrence of multiple TonB proteins in many Gram-negative bacteria suggests that similar mechanisms may operate for atypical TBDT substrates.

MATERIALS AND METHODS

Bacterial strains and media. *E. coli* was grown in LB broth or plated on LB agar and grown at 37°C. DH5α and BL21(DE3) strains were used as host strains for cloning and for IPTG-induced protein expression, respectively. *P. carotovorum* was grown in LB broth or plated on LB agar at 30°C with the addition of the iron chelator 2,2′-bipyridine where specified. LB media and agar for culturing plasmid-complemented deletion strains always contained 100 μg ml^{-1} ampicillin.

Generation of gene knockout strains and plasmids. The *fusA* (KAA3668913), *fusB* (KAA3668912), *fusC* (KAA3668914), and *tonB* (KAA3668374) sequences were determined from the genome sequence of *P. carotovorum* LMG2410 (GenBank BioProject accession no. PRJNA543207) (28). Genes of *Pc*LMG2410 were deleted using the lambda red method as described previously (11, 29). The primers used for amplifying the kanamycin cassette from pKD4 template plasmid and gene sequences from genomic DNA and for plasmid site-directed mutagenesis are listed in Table S1 in the supplemental material. The gene knockouts were confirmed by PCR and sequencing. Table S2 shows all the plasmids used in this study. To construct all of the plasmids, except pFusANTR-GFP, the respective genes were amplified from wild-type genomic DNA using primers that contained flanking regions with NdeI (forward) and XhoI (reverse) restriction enzyme sites. Purified PCR products were digested and ligated into NdeI/XhoI-digested pJ404, which carries ampicillin resistance. To generate pFusANTR-GFP, the sequence encoding the N-terminal portion of FusA was amplified with primers containing XhoI (forward) and BamHI (reverse) restriction enzyme sites and the PCR products were inserted into XhoI/BamHI-digested pWaldo plasmid (30). The complementation plasmids were transformed into competent LMG2410 knockout strains by electroporation.

Protein production and purification. FusC, FusB$_{CTD}$, TonB$_{CTD}$, FusA$_{NTR}$-GFP, and all ferredoxin proteins were overproduced in *E. coli* and purified as described previously (11, 12), with the exception of spinach ferredoxin (Fer$_{Sp}$), which was purchased from Sigma. GFP alone used as a negative control in ITC was produced by cleavage of FusA$_{NTR}$-GFP with tobacco etch virus (TEV) protease for 2 h at room temperature (RT) at a 50:1 ratio. The resulting GFP-His$_8$ was separated from residual TEV protease by size exclusion chromatography, and the removal of the N-terminal region of FusA was confirmed by SDS-PAGE.

Growth enhancement assays. Growth enhancement in the presence of ferredoxin was performed on solid media as previously described (11). Briefly, 10 ml of 0.8% precooled agar was supplemented with 50 μl of mid-log culture in LB media and poured onto an LB agar base containing 400 μM 2,2′-bipyridine (and 0.2 mM IPTG where specified). For plasmid based complementation, Ampicillin (100 μg/ml) was added to the LB media base. A 4-μl volume of ferredoxin was spotted onto the solidified plate at the specified concentration. For growth enhancement in liquid media, bacteria were grown in M9 minimal media. Cultures (10 ml) were inoculated with a 1-in-50 dilution of overnight LB cultures and, upon reaching an optical density at 600 nm (OD$_{600}$) of 0.45, were supplemented with 0.2 μM Fer$_{Ara}$, and growth was monitored by measuring the OD$_{600}$ for 6 h.

Ferredoxin internalization and depletion assays. All experiments were repeated at least once. The time course of ferredoxin internalization was initiated by supplementing LB cultures of wild-type or $\Delta fusC$ cells (OD$_{600}$ of 0.5) with 2,2′-bipyridine to reach a final concentration of 200 μM. Fer$_{Ara}$ or Fer$_{Pot}$ was added to reach a final concentration of 1 μM, and the cultures were grown at 30°C with shaking over the specified time. At each time point, a volume equivalent to 1 ml of cell suspension at OD$_{600}$ of 0.5 was removed and the cells were spun down and treated with BugBuster (Merck) for extraction of soluble protein. To determine if the $\Delta fusA$ and $\Delta fusB$ strains could take up ferredoxin, LB cultures of WT and deletion strains at an OD of ~0.5 were supplemented with 200 μM 2,2′-bipyridine and 1 μM *Arabidopsis* or 5 μM potato ferredoxin. After 2 h at 30°C with shaking, 1 ml of cells was pelleted and soluble proteins were extracted using BugBuster (Merck). For internalization experiments involving plasmid-complemented deletion strains, LB cultures were grown until an OD$_{600}$ of 0.4 was reached, whereupon 2,2′-bipyridine and potato ferredoxin were added. $\Delta fusA$+pFusA and $\Delta fusB$+pFusB cultures were split into two separate tubes, one of which was supplemented with IPTG to reach a final concentration of 0.2 mM. After 2 h, cells were harvested and subjected to BugBuster extraction as described above.

Depletion of *Arabidopsis* ferredoxin was monitored in 2 ml M9 minimal medium cultures of WT, $\Delta fusA$, and $\Delta fusB$ strains over the course of 4 h. Each culture, as well as 2 ml of uninoculated media (negative control), was supplemented with 100 μM 2,2′-bipyridine and 1 μM Fer$_{Ara}$. At each time point, 50 μl of culture was removed from each tube, and after the cells were pelleted, the supernatant was mixed with SDS loading dye.

The effect of dissipating PMF on ferredoxin uptake was determined using protonophore CCCP (Sigma), which was dissolved in dimethyl sulfoxide (DMSO) to reach a final concentration of 10 mM. Mid-log cultures of wild-type and $\Delta fusC$ *Pc*LMG2410 in M9 media were supplemented with 300 μM 2,2′-bipyridine, and 2 ml of each culture was mixed with 18 μl DMSO and 2 μl CCCP stock (for a 10 μM CCCP final concentration) or 20 μl CCCP stock (for a 10 μM final CCCP concentration) or with 20 μl DMSO alone for the "no-CCCP" control. The cultures were mixed and incubated at room temperature for 10 min, after which the wild-type cultures were supplemented with 1 μM Fer$_{Pot}$ and the $\Delta fusC$ cultures with 0.2 μM Fer$_{Ara}$. After 45 min of incubation at 30°C with shaking, 1 ml of each culture was pelleted, washed with 0.5 ml phosphate-buffered saline (PBS), and subjected to BugBuster extraction.

Ferredoxin cleavage assays. Cleavage reactions were performed at RT in a mixture containing 10 mM Tris-HCl (pH 7.5), 50 mM NaCl, 2 μM FusC, and 250 μM ferredoxin. At each time point, a 12-μl volume was removed and mixed with SDS loading dye. Proteins were resolved on a 16% SDS-PAGE gel and visualized by Coomassie staining.

Analytical size exclusion chromatography. Proteins were concentrated to ~600 μM, and 20 μl of TonB$_{CTD}$ or the relevant construct of FusB$_{CTD}$ was mixed with an equal volume of Fer$_{Sp}$. The mixtures were then diluted with SEC buffer (20 mM Tris-HCl [pH 7.5], 150 mM NaCl) to 0.2 ml and loaded onto Superdex 75 10/300 column (GE Healthcare), preequilibrated in the same buffer. Each protein was also passed through the column individually for reference. The chromatograms were recorded at both 280 and 330 nm.

Isothermal titration calorimetry. Experiments were performed on a MicroCal iTC$_{200}$ instrument (Malvern) at 25°C in 10 mM Tris-HCl (pH 7.5)–150 mM NaCl, with a differential power setting of 3. All proteins were dialyzed against the ITC buffer overnight at 4°C with the exception of FusB$_{CTD}$ and TonB$_{CTD}$, which were subjected to gel filtration in ITC buffer immediately before the experiment. Each type of titration was repeated at least once using different batches of purified proteins. Injection volumes of 2 μl were used, and the titrations were continued until the signal corresponded to heat data representing dilution. The magnitude of heat data representing dilution for each titrant was established in a separate experiment, where the titrant was injected into buffer. Dissociation constant (K_d) values are expressed as means ($\pm$ standard errors of the means [SEM]).

SUPPLEMENTAL MATERIAL

Supplemental material is available online only.

FIG S1, JPG file, 0.5 MB.

FIG S2, JPG file, 0.4 MB.

FIG S3, JPG file, 0.8 MB.

FIG S4, JPG file, 0.6 MB.

FIG S5, JPG file, 0.4 MB.
FIG S6, JPG file, 0.2 MB.
FIG S7, JPG file, 0.6 MB.
TABLE S1, DOCX file, 0.01 MB.
TABLE S2, DOCX file, 0.01 MB.

REFERENCES

1. Krewulak KD, Vogel HJ. 2011. TonB or not TonB: is that the question? Biochem Cell Biol 89:87–97. https://doi.org/10.1139/O10-141.
2. Noinaj N, Guillier M, Barnard TJ, Buchanan SK. 2010. TonB-dependent transporters: regulation, structure, and function. Annu Rev Microbiol 64:43–60. https://doi.org/10.1146/annurev.micro.112408.134247.
3. Noinaj N, Easley NC, Oke M, Mizuno N, Gumbart J, Boura E, Steere AN, Zak O, Aisen P, Tajkhorshid E, Evans RW, Gorringe AR, Mason AB, Steven AC, Buchanan SK. 2012. Structural basis for iron piracy by pathogenic Neisseria. Nature 483:53–58. https://doi.org/10.1038/nature10823.
4. Celia H, Noinaj N, Zakharov SD, Bordignon E, Botos I, Santamaria M, Barnard TJ, Cramer WA, Lloubes R, Buchanan SK. 2016. Structural insight into the role of the Ton complex in energy transduction. Nature 538:60–65. https://doi.org/10.1038/nature19757.
5. Maki-Yonekura S, Matsuoka R, Yamashita Y, Shimizu H, Tanaka M, Iwabuki F, Yonekura K. 2018. Hexameric and pentameric complexes of the ExbBD energizer in the Ton system. Elife 7:e35419. https://doi.org/10.7554/eLife.35419.
6. Hickman SJ, Cooper REM, Bellucci L, Paci E, Brockwell DJ. 2017. Gating of TonB-dependent transporters by substrate-specific forced remodelling. Nat Commun 8:14804. https://doi.org/10.1038/ncomms14804.
7. Glenwright AJ, Pothula KR, Bhamidimarri SP, Chorev DS, Baslé A, Firbank SJ, Zheng H, Robinson CV, Winterhalter M, Kleinekathöfer U, Bolam DN, van den Berg B. 2017. Structural basis for nutrient acquisition by dominant members of the human gut microbiota. Nature 541:407–411. https://doi.org/10.1038/nature20828.
8. Gómez-Santos N, Glatter T, Koebnik R, Świątek-Połatyńska MA, Søgaard-Andersen L. 2019. A TonB-dependent transporter is required for secretion of protease PopC across the bacterial outer membrane. Nat Commun 10:1360. https://doi.org/10.1038/s41467-019-09366-9.
9. Kleanthous C. 2010. Swimming against the tide: progress and challenges in our understanding of colicin translocation. Nat Rev Microbiol 8:843–848. https://doi.org/10.1038/nrmicro2454.
10. White P, Joshi A, Rassam P, Housden NG, Kaminska R, Goult JD, Redfield C, McCaughey LC, Walker D, Mohammed S, Kleanthous C. 2017. Exploitation of an iron transporter for bacterial protein antibiotic import. Proc Natl Acad Sci U S A 114:12051–12056. https://doi.org/10.1073/pnas.1713741114.
11. Mosbahi K, Wojnowska M, Albalat A, Walker D. 2018. Bacterial iron acquisition mediated by outer membrane translocation and cleavage of a host protein. Proc Natl Acad Sci U S A 115:6840–6845. https://doi.org/10.1073/pnas.1800672115.
12. Grinter R, Josts I, Mosbahi K, Roszak AW, Cogdell RJ, Bonvin AMJJ, Milner JJ, Kelly SM, Byron O, Smith BO, Walker D. 2016. Structure of the bacterial plant-ferredoxin receptor FusA. Nat Commun 7:6840–6845. https://doi.org/10.1038/ncomms1330.
13. Grinter R, Milner J, Walker D. 2012. Ferredoxin containing bacteriocins suggest a novel mechanism of iron uptake in Pectobacterium spp. PLoS One 7:e33033. https://doi.org/10.1371/journal.pone.0033033.
14. Grinter R, Josts I, Zeth K, Roszak AW, McCaughey LC, Cogdell RJ, Milner JJ, Kelly SM, Byron O, Walker D. 2014. Structure of the atypical bacteriocin pectocin M2 implies a novel mechanism of protein uptake. Mol Microbiol 93:234–246. https://doi.org/10.1111/mmi.12655.
15. Grinter R, Hay ID, Song J, Wang J, Teng D, Dhanesakaran V, Wilksch JJ, Davies MR, Littler D, Beckham SA, Henderson IR, Strugnell RA, Dougan G, Lithgow T. 2018. FusC, a member of the M16 protease family acquired by bacteria for iron piracy against plants. PLoS Biol 16:e2006026. https://doi.org/10.1371/journal.pbio.2006026.
16. Neupert W, Brunner M. 2002. The protein import motor of mitochondria. Nat Rev Mol Cell Biol 3:555–565. https://doi.org/10.1038/nrm878.
17. Backes S, Herrmann JM. 2017. Protein translocation into the intermembrane space and matrix of mitochondria: mechanisms and driving forces. Front Mol Biosci 4:83. https://doi.org/10.3389/fmolb.2017.00083.
18. Kasianowicz J, Benz R, McLaughlin S. 1984. The kinetic mechanism by which CCCP (carbonyl cyanidem-chlorophenylhydrazone) transports protons across membranes. J Membrain Biol 82:179–190. https://doi.org/10.1007/BF01868942.
19. Braud A, Hannauer M, Mislin GLA, Schalk IJ. 2009. The Pseudomonas aeruginosa pyochelin-iron uptake pathway and its metal specificity. J Bacteriol 191:3517–3525. https://doi.org/10.1128/JB.00010-09.
20. Shultis DD, Purdy MD, Banchs CN, Wiener MC. 2006. Outer membrane active transport: structure of the BtuB:TonB complex. Science 312:1396–1399. https://doi.org/10.1126/science.1127694.
21. Ferguson AD. 2002. Structural basis of gating by the outer membrane transporter FecA. Science 295:1715–1719. https://doi.org/10.1126/science.1067313.
22. Cardoso de Amorim G, Prochnicka-Chalufour A, Delepelaire P, Lefèvre J, Simenel C, Wandersman C, Delepierre M, Izadi-Pruneyre N. 2013. The structure of HasB reveals a new class of TonB protein fold. PLoS One 8:e58964. https://doi.org/10.1371/journal.pone.0058964.
23. Peacock RS, Weljie AM, Howard SP, Price FD, Vogel HJ. 2005. The solution structure of the C-terminal domain of TonB and interaction studies with TonB box peptides. J Mol Biol 345:1185–1197. https://doi.org/10.1016/j.jmb.2004.11.026.
24. Schauer K, Rodionov DA, de Reuse H. 2008. New substrates for TonB-dependent transport: do we only see the 'tip of the iceberg'? Trends Biochem Sci 33:330–338. https://doi.org/10.1016/j.tibs.2008.04.012.
25. López CS, Peacock RS, Crosa JH, Vogel HJ. 2009. Molecular characterization of the TonB2 protein from the fish pathogen Vibrio anguillarum. Biochem J 418:49–59. https://doi.org/10.1042/BJ20081462.
26. Paquelin A, Ghigo JM, Bertin S, Wandersman C. 2001. Characterization of HasB, a Serratia marcescens TonB-like protein specifically involved in the haemophore-dependent haem acquisition system. Mol Microbiol 42:995–1005. https://doi.org/10.1046/j.1365-2958.2001.02628.x.
27. Cascales E, Buchanan SK, Duché D, Kleanthous C, Lloubès R, Postle K, Riley M, Slatin S, Cavard D. 2007. Colicin biology. Microbiol Mol Biol Rev 71:158–229. https://doi.org/10.1128/MMBR.00036-06.
28. Rooney WM, Wojnowska M, Walker D. 2019. Draft genome sequence of the necrotrophic plant-pathogenic bacterium Pectobacterium carotovorum subsp. carotovorum strain LMG 2410. Microbiol Resour Announc 8:e00614-19. https://doi.org/10.1128/MRA.00614-19.
29. Datsenko KA, Wanner BL. 2000. One-step inactivation of chromosomal genes in Escherichia coli K-12 using PCR products. Proc Natl Acad Sci 97:6640–6645. https://doi.org/10.1073/pnas.120163297.
30. Waldo GS, Standish BM, Berendzen J, Terwilliger TC. 1999. Rapid protein-folding assay using green fluorescent protein. Nat Biotechnol 17:691–695. https://doi.org/10.1038/10904.